# Benchmark Data for Evaluation of NASA Impedance Eduction Methods

M. G. Jones*, B. M. Howerton†
*NASA Langley Research Center, Hampton, VA 23681*

**Results achieved with three acoustic liner configurations are used to evaluate the effects of recent modifications to the NASA Normal Incidence Tube and Grazing Flow Impedance Tube. These include a calibration liner, a wire mesh liner, and a perforate liner. The effects of source type, source level, and mean flow Mach number on the impedances educed with these liners are explored. Existing models are used to predict the impedance for each test condition, and are compared with educed impedance spectra to determine their validity. The results suggest that educed impedances are similar for either a stepped sine or swept sine source. The predicted models are acceptable for the perforate liner, and are quite good for the calibration and wire mesh liners.**

## I. Introduction

Acoustic liners are used extensively throughout the aircraft nacelle inlet and aft-bypass duct to absorb tonal (e.g., noise due to rotor-alone and rotor-stator interaction) and broadband (e.g., noise due to turbulent flow through the nacelle) noise generated by the fan in commercial subsonic aircraft. Although these liners provide significant fan noise reduction, there is continual pressure to develop improved liner concepts in order to meet the ever-tightening noise restrictions imposed by the International Civil Aviation Organization (ICAO) and the Federal Aviation Administration (FAA) for commercial aircraft. A key parameter in the development of improved acoustic liners is acoustic impedance, which is the ratio of the Fourier transforms of the acoustic pressure and the normal component of acoustic particle velocity time histories at a point of interest (e.g., at the surface of the liner).[1]

The NASA Langley Research Center has developed multiple test rigs for use in the eduction (inference) of acoustic impedance.[2] Two of the more commonly used test rigs are the Normal Incidence Tube (NIT) and Grazing Flow Impedance Tube (GFIT). The NIT supports evaluation of acoustic liners over a range of frequencies and source sound pressure levels (SPLs) in the absence of flow. Complex acoustic pressures measured at two distances from the liner surface are used to compute the acoustic impedance of the liner. The GFIT allows the effects of tangential mean flow to be taken into account, albeit via a more complicated computational analysis. Complex acoustic pressures acquired along the wall opposite the liner are used to educe the acoustic impedance of the liner.

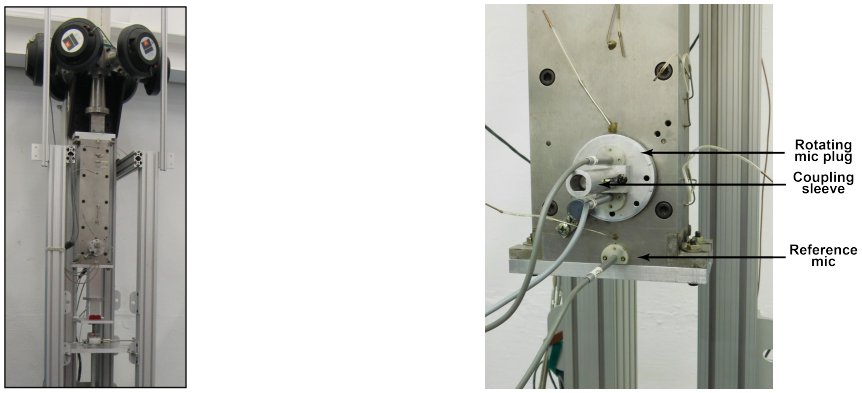
The purpose of this study is three-fold. The first goal is to acquire data in both test rigs using a set of common liners: (1) a calibration liner, (2) a wire mesh liner, and (3) a conventional perforate liner. These liners are chosen to cover a range of linearity (sensitivity to source SPL). Data are acquired in the NIT and GFIT with different source types and multiple source SPLs, frequencies, and mean flow Mach numbers. The second goal of this study is to compare acoustic impedance spectra measured with these two test rigs. The Two-Microphone Method[2–4] and Prony Method[5,6] are used with NIT and GFIT data, respectively. The third goal is to compare the educed impedances with those predicted using two impedance prediction codes, ZKTL[7] and TPM.[8] The surface impedance spectra for the calibration and wire-mesh liners should be predictable from first principles, whereas the models used to predict the impedance for the conventional perforate liner are semiempirical. Finally, these data will be made available to the public to enable others to compare their respective analysis techniques with the NASA results on a common database.

*Senior Research Scientist, Research Directorate, Structural Acoustics Branch, AIAA Associate Fellow.
†Research Scientist, Research Directorate, Structural Acoustics Branch, AIAA Senior Member.

This paper is organized into seven sections. Sections II and III provide descriptions of the test rigs and test liners. Sections IV and V present the impedance eduction and prediction methods used to evaluate these test liners. Results are presented in Section VI, and key findings are summarized in Section VII.

## II. NASA Test Rigs

Figure 1 provides a photograph of the NASA Normal Incidence Tube (NIT). This device uses six 120 W compression acoustic drivers to produce a sound field that impinges on the surface of the acoustic liner. The 2"×2" waveguide is approximately 36" long and contains three flush-mounted microphones. A reference microphone located 0.25" from the surface of the liner is used to ensure that the liner is exposed to the desired sound pressure level (SPL). Two measurement microphones are positioned 2.50" and 3.75" from the liner surface, and are mounted within a rotating plug such that their positions can be precisely interchanged. This capability is of particular value for the Two-Microphone Method,[3,4] in that it allows intrinsic amplitude and phase errors due to mismatched calibrations of the two microphones to be eliminated.




(a) Full NIT. (b) Close-up view of measurement section.

Figure 1: NASA Normal Incidence Tube (NIT).

Two source types are considered, stepped sine and swept sine. For the former, tones at selected frequencies (0.1 kHz increment) are tested one at a time. A controlled-amplitude, swept-sine source[9] allows the source magnitude to be maintained to within ±0.5 dB of the target while the frequency is swept through the range of interest. This method provides data at approximately 5 Hz increments over the frequency range of 0.4 to 3.0 kHz. Data are acquired at source levels of 100, 120, and 140 dB to allow evaluation of the effects of liner nonlinearity.

The NASA Langley Grazing Flow Impedance Tube (GFIT, Fig. 2) has a cross-sectional geometry of 2.0"-wide by 2.5"-high, and allows evaluation of acoustic liners with lengths from 2.0" to 24.0". The surface of the test liner forms a portion of the upper wall of the flow duct. Twelve acoustic drivers form an upstream (exhaust mode) source and six acoustic drivers form a downstream (inlet mode) source. Exhaust mode data are used for the current investigation.

The same source types are employed for the GFIT, except the frequency resolution for the swept-sine source is set to 10 Hz. Data are acquired at frequencies of 0.4 to 3.0 kHz and at centerline Mach numbers of 0.0, 0.3, and 0.5 (Mach 0.5 data will be made available, but are not presented herein for the sake of brevity). There are 95 microphones mounted in the rigid walls of the waveguide, with 53 flush-mounted in the lower wall (opposite the liner) of the GFIT. Acoustic pressures measured with these lower-wall microphones are used with the Prony Method to educe the impedance of the test liner.

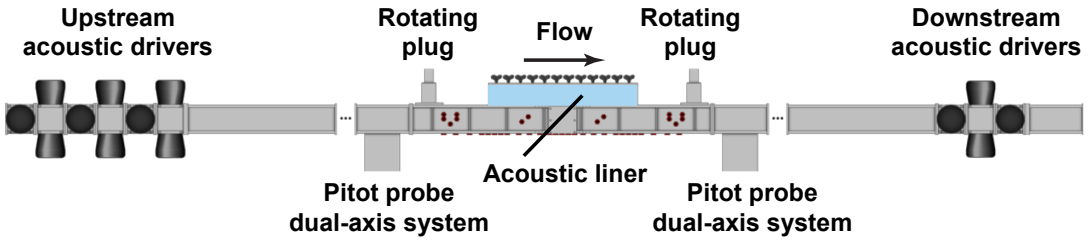
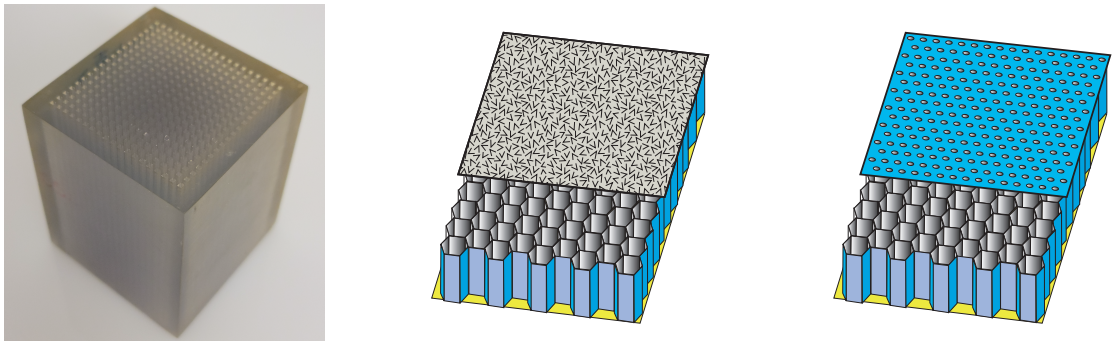



Figure 2: Sketch of Grazing Flow Impedance Tube (GFIT).

## III. Acoustic Liners

Three liner configurations were considered (Fig. 3) for this investigation. Two samples were constructed for each configuration to allow testing in the NIT and GFIT.



(a) Calibration liner. (b) Wire mesh liner. (c) Perforate liner.

Figure 3: Sketches of test liners.

The first configuration, labeled CSQ3, is comprised of 0.05"×0.05" square chambers with a core depth of 3.0" (Fig. 3a). The NIT version of this liner consists of a 19×19 array of chambers distributed over a 2"×2" active surface, providing an open area ratio of 0.22. No facesheet is required because of the small diameter of the chambers. Instead, acoustic resistance is achieved via viscous losses along the inner walls. The GFIT version of the CSQ3 consists of eight replications of the active portion (19×19 array) of the NIT geometry, and has a total liner length of 16". The CSQ3 liner is labeled as a "calibration liner" because it can be easily modeled using the ZKTL model (Sec. V). Also, the chamber length to diameter ratio is greater than 50, which causes the liner to exhibit linear behavior (i.e., minimal effects of source SPL or tangential flow on the surface impedance).

The second configuration consists of a wire mesh facesheet mounted over a core (Fig. 3b). The NIT version of this liner, labeled E15R27, consists of a piston sleeve adjusted to provide an empty core depth of 1.5" with a rigid backplate. A 27 cgs rayl wire mesh is mounted to the surface of the piston sleeve via double-back tape to minimize vibration. Since this sample has a cross section of 2"×2", only plane waves are present within the core over the frequency range of interest (up to 3.0 kHz). Therefore, honeycomb core material is not required to ensure local reaction. The corresponding GFIT version of the wire mesh liner, labeled C1R27, has a 2.0"×23.5" active surface and contains 1.5"-deep conventional honeycomb core mounted over a rigid backplate. The diameter of the core chambers is approximately 0.375". The 27 cgs rayl wire mesh material is used as the facesheet for this liner.

The last configuration considered is the conventional perforate liner (see Fig. 3c). Nearly all acoustic liners currently used in commercial aircraft are constructed in this manner. Depending on the particular

application, there may also be a porous septum embedded within the core, but this configuration was not included in the current study. NIT and GFIT versions of a perforate liner, labeled GE01, were used in this study. Each of these liners has a 1.5"-deep honeycomb core (same as used for the wire mesh liner) covered by a perforated facesheet. This 0.025"-thick facesheet has 0.039"-diameter perforations and an open area ratio of 0.087. The NIT version has a 2"×2" active surface, and the GFIT has a 2"×16" active surface.

## IV. Impedance Eduction Methods

The Two-Microphone Method[2–4] is used with data acquired in the NIT to determine the impedance at the surface of the test liner. This method requires acoustic pressures to be measured at two prescribed distances from the liner surface (Fig. 1). A switching method is employed via a stepper motor to precisely interchange the locations of the two microphones, which are flush-mounted within a rotating plug. The acoustic pressures are measured with the two microphones in one orientation, the plug is rotated, and the acoustic pressures are measured again with the microphone locations in the reverse orientation. The two sets of readings are geometrically averaged, taking into account the respective orientations, to determine the true acoustic pressures at each location. These acoustic pressures are used to separate the incident and reflected (from the surface of the liner) signals, thereby allowing the impedance of the test liner to be computed.

The Prony Method used with GFIT data is based on de Prony's original analysis.[10] It assumes the liner has infinite length and the sound field is unidirectional. As such, reflections at the leading and trailing edges of the liner are neglected in the analysis. Application of this method for liner impedance eduction has been described in earlier papers.[5,6] The axial wavenumber is determined from the acoustic pressures measured with the microphones on the wall opposite the uniform-impedance liner. This wavenumber is input to the Myers impedance boundary condition[11] to compute the impedance of the test liner.

## V. Impedance Prediction Methods

Different impedance prediction methods are used for each liner type. The Zwikker-Kosten Transmission Line Method (ZKTL)[7] is used for the calibration liner. This method uses a transmission line model based on the analysis of Zwikker and Kosten[12] to predict the acoustic impedance of an individual liner chamber. The calculation starts with a rigid-wall backplate assumption, then marches through the individual layers of the liner to compute the acoustic pressure and velocity at the surface of the liner, from which the impedance can be computed. The transmission line calculations are based on the characteristic impedance and propagation constant of each layer, which can be easily calculated based on the liner geometry.

The impedance of wire mesh liners is found from first principles. The wire mesh liners are comprised of a wire mesh facesheet and a core. The core is empty for the NIT samples, and is filled with conventional honeycomb material for the GFIT sample. Given the diameter of the core chambers (approximately 0.375"), the acoustic resistance achieved via viscous losses along the chamber walls is negligible. Thus, the resistance of the liner is almost entirely provided by the wire mesh. The wire mesh provides negligible mass reactance, so the reactance of the liner is based on the cavity depth. As such, the surface impedance, $\zeta_{\mathrm{wm}}$, for a wire mesh liner is well described by

$$\zeta_{\mathrm{wm}} = \frac{R_f}{\rho c} - i \cot\left(kD\right), \tag{1}$$

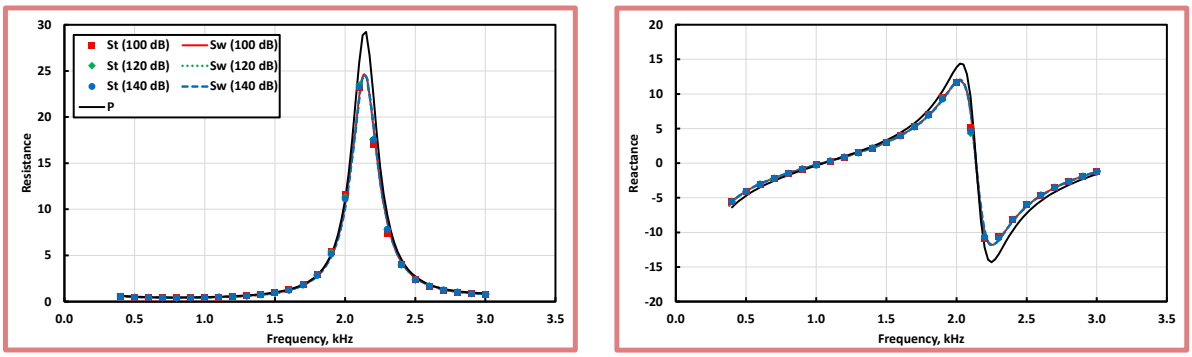
where $R_f$, $k$, and $D$ are the DC flow resistance of the wire mesh, the freespace wavenumber, and the core depth, respectively, and $\rho$ and $c$ are the density and sound speed of air. (An $e^{i\omega t}$ time convention is assumed throughout this paper.)

Finally, the Two-Parameter Model (TPM)[8,13] is used for prediction of the impedance change across a perforate facesheet. This model seeks to account for viscous, nonlinear, and grazing flow contributions to the facesheet resistance. The perforate facesheet is treated as a lumped element, such that the acoustic oscillatory flow through the perforate can be treated as locally incompressible and quasisteady.

The first two methods (ZKTL and Equation [1]) are linear calculations, i.e., independent of source level. However, the TPM employs a nonlinear calculation and therefore requires the source level to be specified.

## VI. Results

Figures 4 - 6 present impedance spectra educed with three liners (CSQ3, E15R27, GE03) mounted in the NIT. Each figure contains results educed from stepped sine and swept sine data (denoted as St and Sw, respectively) acquired at source levels of 100, 120, and 140 dB. Predicted impedances (denoted as P) are also included. All impedances are normalized by the quantity $\rho c$ in this paper.

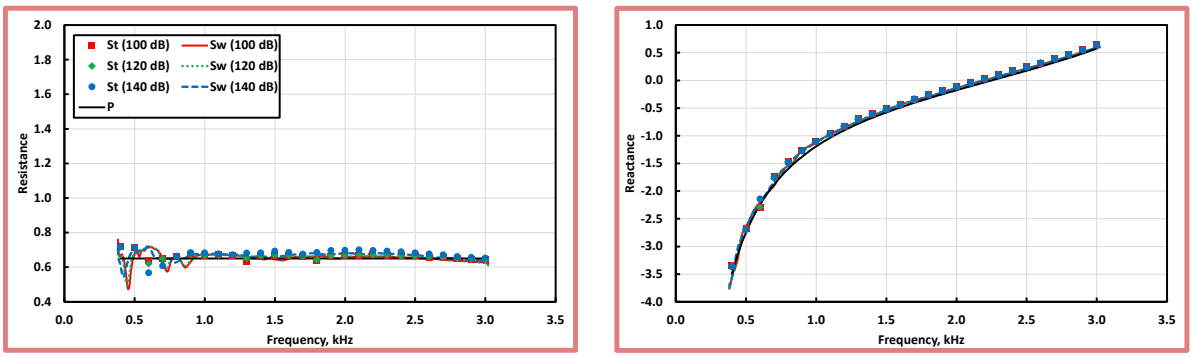



(a) Normalized Resistance.

(b) Normalized Reactance.

Figure 4: Comparison of predicted (P) and educed impedance spectra - CSQ3 liner in NIT. **St** and **Sw** represent impedances educed with stepped and swept sine data, respectively.

The first result is for the calibration liner, CSQ3 (Fig. 4). As shown in Figure 3a, the chambers are quite small and there is no facesheet. Hence, the viscous losses along the walls of these chambers are responsible for the majority of the liner resistance. As expected, the reactance follows a classical $-\cot(kD)$ pattern. Because of the large depth of these chambers (3.0"), antiresonance occurs near 2.1 kHz, with a corresponding strong peak in resistance. Differences between the results attained with two source types and over this wide range of source SPLs are negligible; i.e., this liner is linear over this regime. The educed and predicted impedances compare favorably except for frequencies near the strong antiresonance (approximately 2.1 kHz). This deviation near antiresonance is expected. The liner is a poor absorber at frequencies where the magnitude of the impedance becomes large, which introduces potential error into the impedance eduction process. However, impedances educed at these frequencies are generally of less importance because of this poor absorption.




(a) Normalized Resistance.

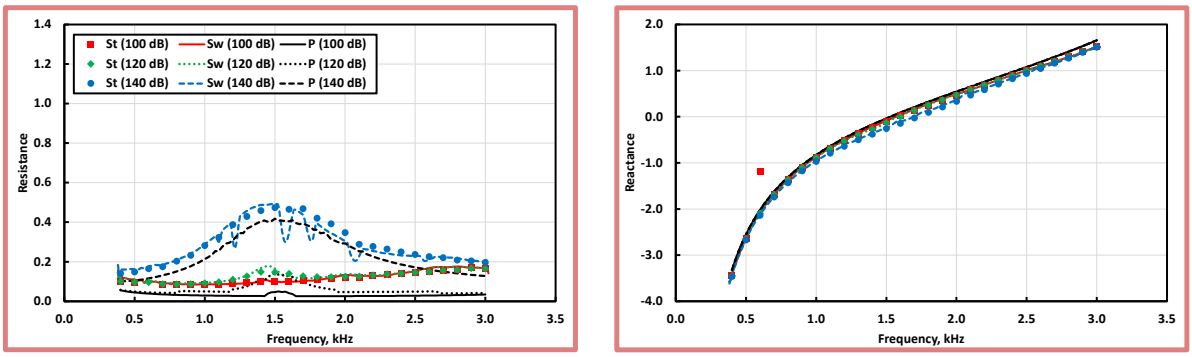
(b) Normalized Reactance.

Figure 5: Comparison of predicted and educed impedance spectra - E15R27 liner in NIT.

Corresponding results for the 1.5"-deep wire mesh liner are presented in Figure 5. Note that although there are perceptible differences between the results attained over this wide range of source SPLs, this liner is also very linear. As noted earlier, the resistance for this liner is provided by the wire mesh with DC

flow resistance of 27 cgs rayls. This corresponds to a frequency-independent normalized resistance of 0.65. Although there is some scatter in the educed resistance spectra at the lower frequencies, the educed and predicted resistance spectra compare favorably over the full frequency range. Scatter in the low-frequency data has been addressed in earlier studies,[14] where it was demonstrated that poor attenuation reduces the efficacy of the impedance eduction process. Specifically, this scatter could be reduced if the core depth was adjusted to move resonance closer to this frequency range, albeit with a corresponding increase in scatter at some other portion of the frequency range. As expected, the reactance follows a classical $-\cot(kD)$ pattern.

Figure 6 presents results for the GE01 conventional perforate liner. Again, due to the chamber diameter, minimal resistance is provided by viscous losses along the chamber walls and the resistance is mostly due to the perforate facesheet. Two key results are readily apparent in the resistance data. First, although the predicted resistance spectra track the educed resistance spectra reasonably well (note the reduced scale), the predicted values are consistently lower. However, the comparison becomes more favorable for the 140 dB data.




(a) Normalized Resistance.

(b) Normalized Reactance.

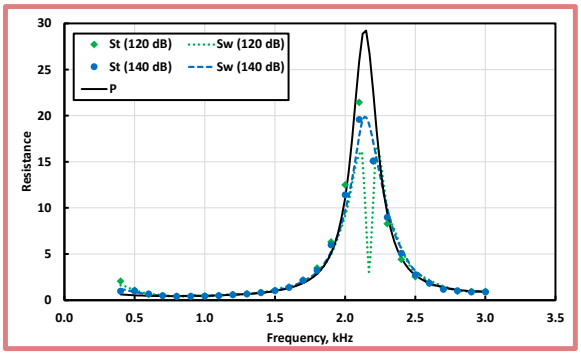
Figure 6: Comparison of predicted and educed impedance spectra - GE01 liner in NIT.

Also, the educed results are virtually independent of the source type (stepped and swept sine). The nonlinearity of this configuration is readily apparent. An increase of the source SPL from 100 to 120 dB has limited effect on the resistance, but an increase to 140 dB causes a noticeable increase in the resistance spectrum. As is generally the case, the reactance spectrum is much less sensitive to changes in the source SPL and, with the exception of an anomalous result at 2.1 kHz, the educed and predicted reactance spectra compare favorably.

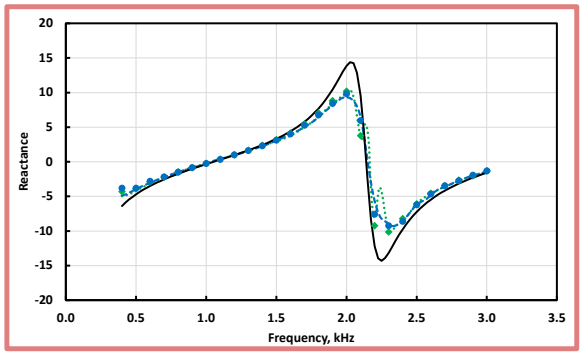
Figures 7 - 9 present results for data acquired in the GFIT at Mach 0.0 with source SPLs of 120 and 140 dB. These results should be very similar to those educed from NIT data, with a few key differences. First, an acoustic pressure plane wave impinges uniformly onto the entire surface of the NIT sample at the prescribed source level. This same source level is present at the leading edge of the liner in the GFIT. However, attenuation over the length of the liner can cause nonlinear effects to become evident with changing SPL. It should be noted that the Prony Method assumes the liner to present a uniform impedance. If the liner is perfectly linear, changes in SPL over the length of the liner should have limited effect on the educed impedance.

Another key difference is in the approach used to perform the impedance eduction. The Prony Method assumes the liner to have infinite length, such that there are no reflections from the leading and trailing edges of the liner or from the upstream and downstream terminations of the duct. Deviations from this assumption cause the impedance eduction process to become less robust. Also, it is important to note that there may be slight manufacturing differences between the NIT and GFIT samples.

The Mach 0.0 GFIT results for the CSQ3 liner (Fig. 7) are very similar to those acquired in the NIT (Fig. 4). The effects of source type and source SPL on the educed impedances are negligible, and the largest deviations from the predicted values occur near antiresonance (recall the limitations due to poor attenuation). Otherwise, the comparison of predicted and educed impedances is very good, albeit slightly less favorable than was observed with the NIT data.



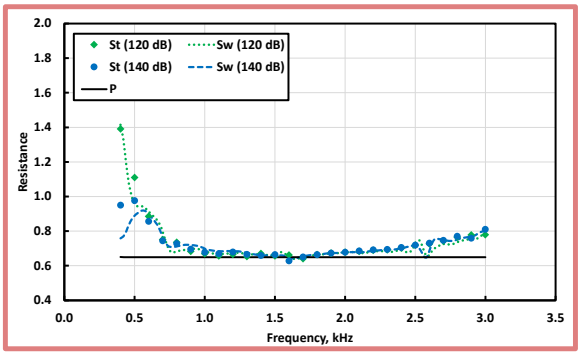

(a) Normalized Resistance.



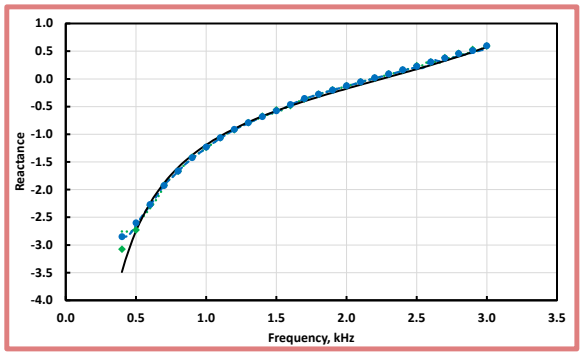

(b) Normalized Reactance.

Figure 7: Comparison of predicted and educed impedance spectra - CSQ3 liner in GFIT, Mach 0.0.

Source type and source SPL effects remain minimal for the C1R27 liner (Fig. 8), confirming the linearity of the sample. However, there is slightly increased separation relative to the NIT results shown in Fig. 5 (note the small scale of this figure) between the predicted and educed resistance spectra at the lower and upper extremes of the frequency range. Recall that there are eduction limitations due to poor attenuation at the lower frequencies. Note also that the C1R27 liner contains honeycomb core, whereas the E15R27 liner had an empty core. Regardless, the comparison is quite favorable. Again, the educed and predicted reactance spectra are nearly identical.




(a) Normalized Resistance.




(b) Normalized Reactance.

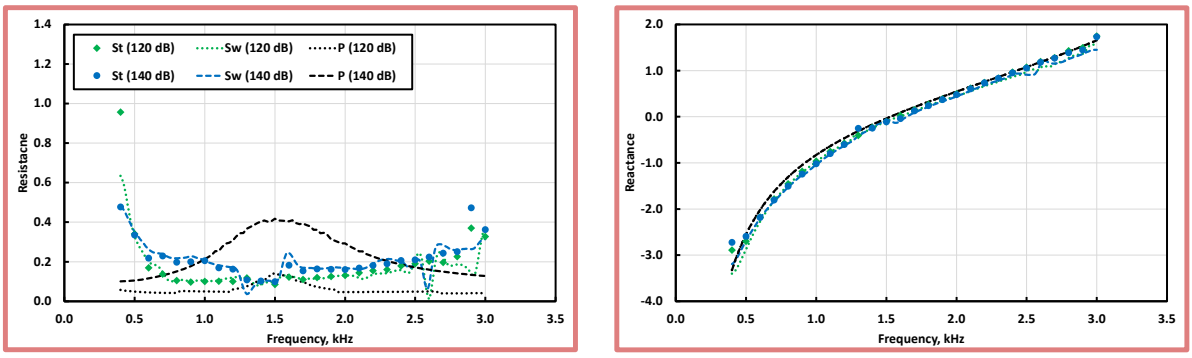
Figure 8: Comparison of predicted and educed impedance spectra - C1R27 liner in GFIT, Mach 0.0.

The corresponding GE01 results are presented in Figure 9. Again, the stepped sine and swept sine source results compare favorably. The resistance spectra educed for a source level of 140 dB are slightly higher than those for a 120 dB source, but the difference is less than that observed with the NIT data.

Note the strong difference between the predicted (black dashed line) and educed (blue dashed line) resistance spectra for the 140 dB case, especially for frequencies near resonance where the impedance eduction process would be expected to provide quality results. Recall that the Prony Method assumes the liner to present a uniform impedance over the length of the liner. This assumption is valid for a linear liner, where the impedance is independent of the SPL present at the liner surface (this explains the favorable comparisons seen in Figures 7 and 8). However, attenuation over the length of a nonlinear liner such as the GE01 causes the SPL to continuously decrease, and this attenuation may be significant for frequencies near resonance. When this occurs, the impedance of this nonlinear liner will also change over the length of the liner. Since the Prony Method treats the entire liner as having a single uniform impedance, this educed impedance should be expected to be a 'weighted average' of the impedances present over different portions of the liner. Thus, since the attenuation for the GE01 liner (140 dB case) is driving the SPL toward (or perhaps below) 120 dB,

the impedance educed with the Prony Method approaches that predicted for a liner subjected to a 120 dB sound field (black dotted line).

Similarly, the resistance educed for the test with a 120 dB source should compare more favorably with the prediction for a liner subjected to a 100 dB sound field. However, recall that the 100 and 120 dB predictions are quite similar (linear regime), so this effect is less pronounced. While there is a slight separation from the prediction, the educed reactance spectra are relatively unaffected by changes in the source level.

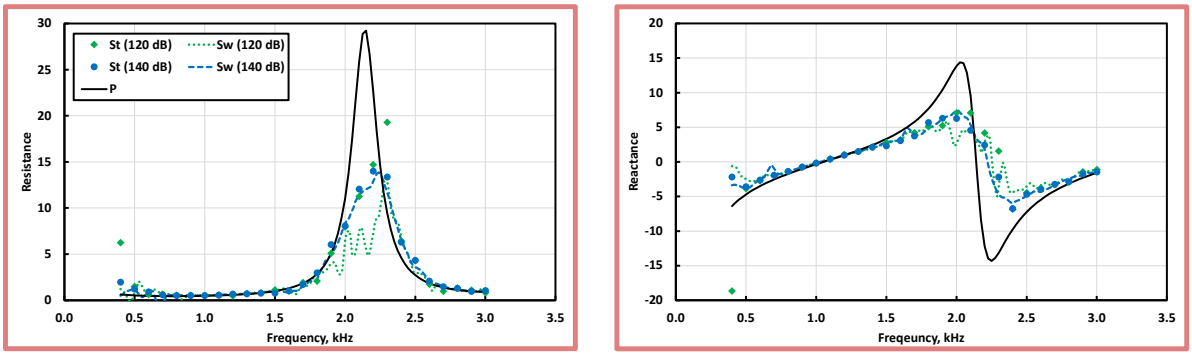



(a) Normalized Resistance.

(b) Normalized Reactance.

Figure 9: Comparison of predicted and educed impedance spectra - GE01 liner in GFIT, Mach 0.0.

Figures 10 - 12 present the corresponding GFIT results acquired with Mach 0.3 tangential flow. Recall that the ZKTL model that is used to predict the impedance for the CSQ3 liner does not include effects of source SPL or mean flow. Thus, the favorable comparison between educed and predicted impedances (away from the antiresonance frequency) confirm that these effects are negligible for this type of liner.




(a) Normalized Resistance.

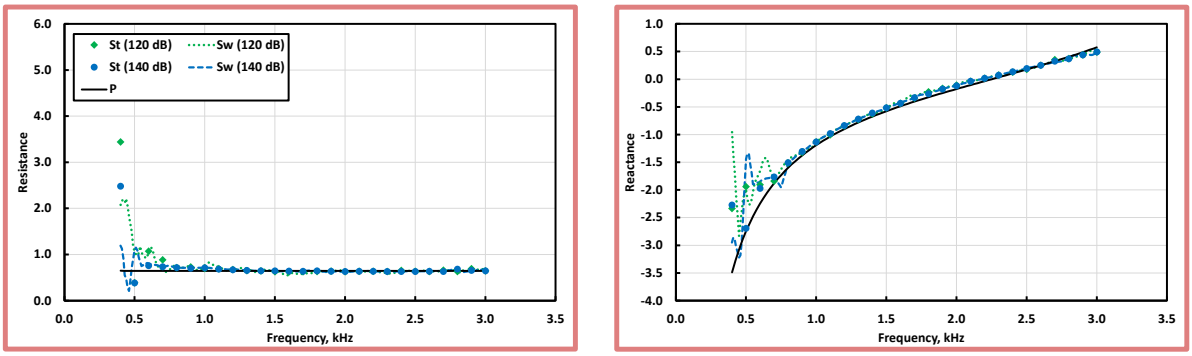
(b) Normalized Reactance.

Figure 10: Comparison of predicted and educed impedance spectra - CSQ3 liner in GFIT, Mach 0.3.

Note the increased scale for the resistance results acquired with the C1R27 liner in Mach 0.3 tangential flow (Fig. 11). This change is needed to allow presentation of the anomalous behavior at the lower frequencies, and therefore tends to obscure small differences between predicted and educed resistance spectra. Nevertheless, the educed and predicted impedances are very similar except at the lowest frequencies (up to about 0.7 kHz).

Again, the perforate liner (Fig. 12) provides interesting results. As shown earlier, there is increased scatter at the lower frequencies. Otherwise, the effects of source type are again demonstrated to be negligible. Perhaps more interesting, the effects of source SPL are also quite minimal. The increase in resistance (predicted and educed values of about 0.7 and 0.8, respectively) due to the mean flow tends to linearize the liner, i.e., reduces the effects of acoustic particle velocity (and thus, the effects of source SPL) on the educed

resistance. It is perhaps useful to note that the amount of attenuation achieved at Mach 0.3 is typically less than that achieved at Mach 0.0. Thus, the effects of attenuation on the impedance eduction process should be subdued. There is also more separation between predicted and educed reactance spectra for this case.

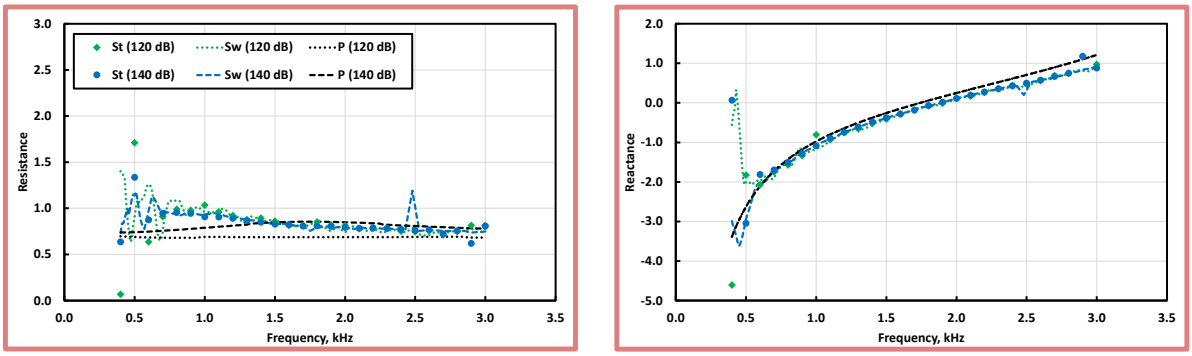



(a) Normalized Resistance.

(b) Normalized Reactance.

Figure 11: Comparison of predicted and educed impedance spectra - C1R27 liner in GFIT, Mach 0.3.

The last set of figures presents comparisons of predicted and measured acoustic pressure profiles. This is the key test for an impedance eduction process, as the main goal is to be able to properly describe the effects of the acoustic liner on the propagated sound field. For each of the three GFIT liners, the measured source and exit plane acoustic pressures and the corresponding liner impedances are used as input to the CHE propagation code[15] to predict the sound pressure and phase axial profiles. These input impedance values are taken from those educed with the Prony Method at 1.0, 1.5, and 2.0 kHz for the Mach 0.3 flow and 140 dB source. Predicted acoustic pressure profiles are compared against the corresponding measured data. In these figures, solid and dotted lines depict predicted and measured results, respectively, and different colors are used for each of the three selected frequencies.




(a) Normalized Resistance.

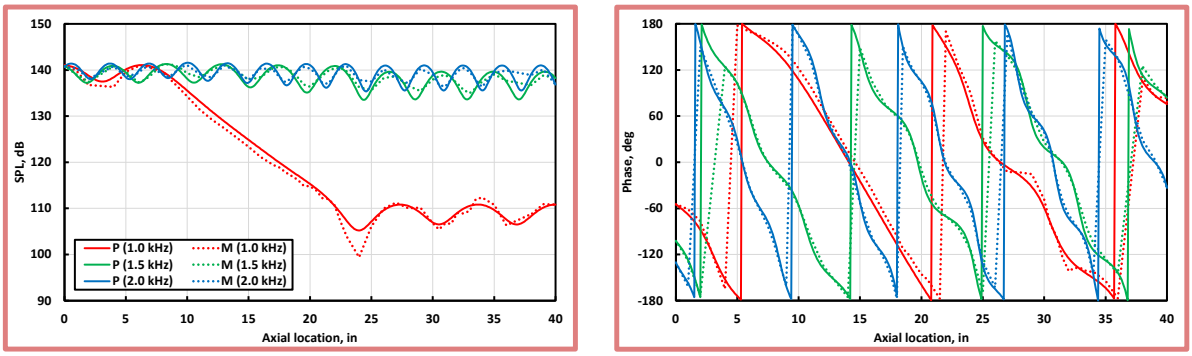
(b) Normalized Reactance.

Figure 12: Comparison of predicted and educed impedance spectra - GE01 liner in GFIT, Mach 0.3.

Figure 13 presents the results for the CSQ3 liner. This liner provides significant attenuation (∼30 dB) at 1.0 kHz. According to the results shown in Figure 10, resonance occurs very near 1.0 kHz, so this result should not be that surprising. Note also that the predicted and measured profiles (both SPL and phase) compare very well. Much less attenuation is observed at 1.5 kHz, and virtually no attenuation occurs at 2.0 kHz (near antiresonance). Nonetheless, the predicted and measured profiles continue to track well.

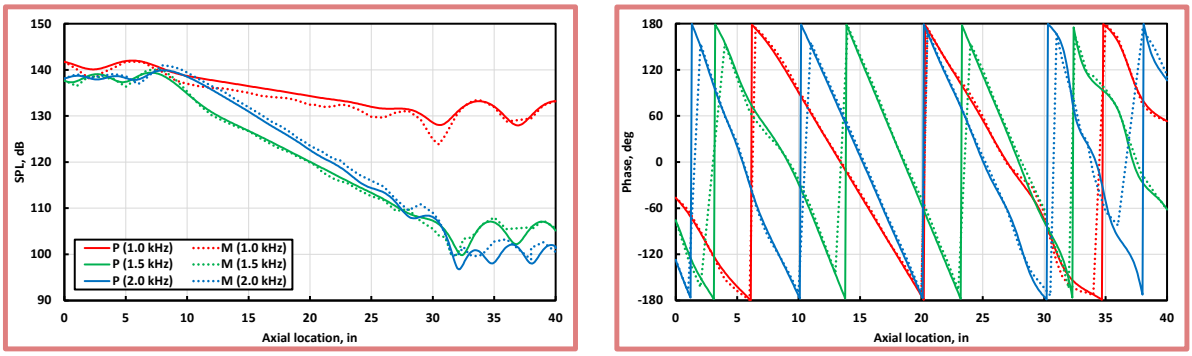
For the wire mesh liner (Fig. 14), excellent attenuation (>35 dB) is achieved at the upper two frequencies, and about 10 dB attenuation is achieved at 1.0 kHz. Favorable comparisons between the predicted and measured results are again observed.

The perforate liner (Fig. 15) also provides good attenuation - approximately 8 dB, 18 dB, and 23 dB at frequencies of 1.0, 1.5, and 2.0 kHz, respectively. Again, the predicted and measured acoustic pressure profiles track very well.



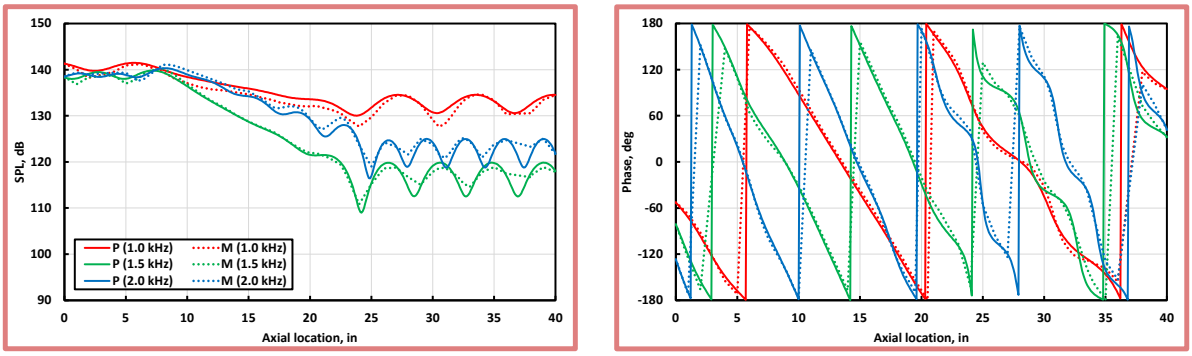

(a) Sound pressure level. (b) Phase.

Figure 13: Predicted (P) and measured (M) acoustic pressure profiles; CSQ3 liner, Mach 0.3, 140 dB source.




(a) Sound pressure level. (b) Phase.

Figure 14: Predicted (P) and measured (M) acoustic pressure profiles; C1R27 liner, Mach 0.3, 140 dB source.




(a) Sound pressure level. (b) Phase.

Figure 15: Predicted (P) and measured (M) acoustic pressure profiles; GE01 liner, Mach 0.3, 140 dB source.

## VII. Concluding Remarks

This paper has presented the results of an ongoing study to evaluate the effects of recent modifications to the NASA Langley Research Center Normal Incidence Tube (NIT) and Grazing Flow Impedance Tube (GFIT). Three liners were evaluated in both test rigs to explore the effects of source type, source level, and mean flow Mach number on the impedance eduction processes. These included a calibration liner, a wire mesh liner, and a conventional perforate liner, chosen to cover a range of linearity. Impedances educed in the NIT and GFIT were compared against impedances predicted with three methods, one for each type of liner. A number of conclusions can be drawn from these results:

1. Good agreement is observed between impedances educed with stepped sine and swept sine sources.
2. The reactance spectra for each of the three test liners is virtually independent of source level, source type, or Mach number.
3. The effects of source SPL up to 140 dB on the educed resistance are neglibile for the calibration and wire mesh liners.
4. The resistance for the perforate liner increases slightly as the source level is increased from 100 to 120 dB, and experiences a more pronounced increase as the level is further increased to 140 dB. An increase from Mach 0.0 to Mach 0.3 causes the resistance to increase further (higher than that attained for 140 dB at Mach 0.0).
5. The impedance eduction process becomes less robust at frequencies with poor attenuation (e.g., near antiresonance).
6. Acoustic pressure profiles predicted with the CHE propagation code, based on impedances educed using the Prony Method, compare favorably with acoustic pressure profiles measured in the GFIT.

It is the intention of the authors to extend this study to include additional liners. These will include additional wire mesh liners to explore the effects of chamber depth on the resonance and corresponding increased attenuation frequency. Additional perforate liners will also be considered to explore the effects of perforate facesheet geometry and corresponding liner nonlinearity on the eduction process, and to further explore the validity of the Two-Parameter Model. Finally, these data will be made available to the public to enable others to compare their respective analysis techniques with the NASA results on a common database.

## Acknowledgements

The authors wish to express sincere appreciation to all those that provided support for this study. Alonzo (Max) Reid and Martha Brown were especially helpful in the data acquisition. This work was funded by the Advanced Air Transport Technology Project of the NASA Advanced Air Vehicles Program.

## References

[1]Blackstock, D. T., *Fundamentals of Physical Acoustics*, Wiley, 2000.

[2]Jones, M. G., Watson, W. R., Nark, D. M., Howerton, B. M., and Brown, M. C., "A Review of Acoustic Liner Experimental Characterization at NASA Langley," NASA TP 220583, April 2020.

[3]Chung, J. Y. and Blaser, D. A., "Transfer function method of measuring in-duct acoustic properties: I. Theory," *Journal of Acoustical Society of America*, Vol. 68, 1980, pp. 907–921.

[4]Jones, M. G. and Stiede, P. E., "Comparison of Methods for Determining Specific Acoustic Impedance," *Journal of the Acoustical Society of America*, Vol. 101, No. 5, May 1997, pp. 2694–2704.

[5]Watson, W. R., Carpenter, M. H., and Jones, M. G., "Performance of Kumaresan and Tufts Algorithm in Liner Impedance Eduction with Flow," *AIAA Journal*, Vol. 53, No. 4, April 2015, pp. 1091–1102.

[6]Jones, M. G., Watson, W. R., and June, J. C., "Optimization of Microphone Locations for Acoustic Liner Impedance Eduction," AIAA Paper 2015-3271, June 2015.

[7]Parrott, T. L. and Jones, M. G., "Parallel-Element Liner Impedances for Improved Absorption of Broadband Sound in Ducts," *Noise Control Engineering Journal*, Vol. 43, No. 6, Nov. 1995.

[8]Parrott, T. L. and Jones, M. G., "Assessment of NASA's Aircraft Noise Prediction Capability, Chapter 6: Uncertainty in Acoustic Liner Impedance Measurement and Prediction," NASA TP 2012-215653, July 2012.

[9]Howerton, B. M., Vold, H., and Jones, M. G., "Application of Sine Sweep Excitation for Acoustic Impedance Eduction," AIAA Paper 2019-2487, May 2019.

[10]de Prony, R., "Essai Éxperimental et Analytique: Sur Les Lois de la Dilatabilité de Fluides Élastique et sur Celles de la Force Expansive de la Vapeur de L'alkool, Àdifférentes Temperatures," *Journal de l'école Polytechnique*, Vol. 1, No. 22, 1795, pp. 24–76.

[11]Myers, M. K., "On the Acoustic Boundary Condition in the Presence of Flow," *Journal of Sound and Vibration*, Vol. 71, No. 3, 1980, pp. 429–434.

[12]Zwikker, C. and Kosten, C., *Sound absorbing materials*, Elsevier Publishing Company, 1949.

[13]Motsinger, R. E. and Kraft, R. E., "Design and Performance of Duct Acoustic Treatment: Aeroacoustics of Flight Vehicles; Chapter 14, Vol. 2: Noise Control," NASA RP 1258, Aug. 1991.

[14]Jones, M. G. and Watson, W. R., "Validation of an Improved Experimental Method for Use in Impedance Eduction," *AIAA Journal*, Vol. 51, No. 1, January 2013, pp. 186–199.

[15]Jones, M. G., Nark, D. M., and Watson, W. R., "Evaluation of a Multizone Impedance Eduction Method," AIAA Paper 2019-2486, May 2019.